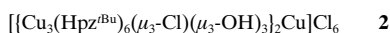
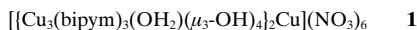


- [4] NH_4XO_4 ($\text{X} = \text{I}, \text{Cl}, \text{Re}$) displays uniaxial NTE: D. Smith, *J. Chem. Phys.* **1983**, *79*, 2995–3001, and references therein.
- [5] Some polymers display uniaxial NTE along the polymer axis, see a) G. Dadobaev, A. I. Slutsker, *Sov. Phys. Solid State* **1981**, *23*, 1131–1135; b) R. M. Barron, T. H. K. Barron, P. M. Mummery, M. Sharkey, *Can. J. Chem.* **1988**, *66*, 718–724; c) R. A. Stobbe, P. C. Hägele, *J. Polym. Sci. Part B* **1996**, *34*, 975–980; d) K. E. Aasmundtveit, E. J. Samuelsen, K. Hoffmann, E. Bakken, P. H. J. Carlsen, *Synth. Met.* **2000**, *113*, 7–18; e) crystals of suberic acid also display uniaxial NTE: Q. Gao, H.-P. Weber, B. M. Craven, R. K. McMullan, *Acta Crystallogr. Sect. B* **1994**, *50*, 695–703.
- [6] TrpGly has been isolated as a fluorescent extract from adult human pituitary glands: S. Partanen, S. Kaakola, I. Kääriäinen, *Acta Physiol. Scand.* **1979**, *107*, 213–218, but its function is still unknown. In mice it produces sedative effects and increases the capacity of diazepam to alleviate leptazol-induced convulsions: S. V. Vellucci, R. A. Webster, *Eur. J. Pharmacol.* **1981**, *76*, 255–259.
- [7] For examples of other peptide nanotubes see a) J. D. Hartgerink, T. D. Clark, M. R. Ghadiri, *Chem. Eur. J.* **1998**, *4*, 1367–1372; b) D. Ranganathan, C. Lakshmi, I. L. Karle, *J. Am. Chem. Soc.* **1999**, *121*, 6103–6107.
- [8] Crystal data: $\text{C}_{13}\text{H}_{15}\text{N}_3\text{O}_3 \cdot \text{H}_2\text{O}$, $M_r = 279.30$, transparent needles, tetragonal, space group $P4_1$ (fixed by known absolute peptide conformation), $Z = 4$. At 295 K: $a = 16.164(3)$, $c = 5.199(1)$ Å, $R_1 = 0.0280$ for 1454 reflections with $F_o^2 > 2\sigma(F_o^2)$ and $R_1 = 0.0285$ for all 1478 data, $S = 1.008$; at 120 K: $a = 16.012(3)$, $c = 5.207(1)$ Å, $R_1 = 0.0315$ for 1802 reflections with $F_o^2 > 2\sigma(F_o^2)$ and $R_1 = 0.0316$ for all 1809 data, $S = 1.016$; MAR345 imaging plate; data reduced with HKL: Y. Otwinowski, W. Minor in *Methods of Enzymology*, Vol. 276 (Eds.: C. W. Carter, Jr., R. M. Sweet), Academic Press, New York, **1997**, pp. 307–326. Solution and refinement were done using SHELXS-97 and SHELXL-97. CCDC-164878 and -164879 contains the supplementary crystallographic data for this paper. These data can be obtained free of charge via www.ccdc.cam.ac.uk/conts/retrieving.html (or from the Cambridge Crystallographic Data Centre, 12, Union Road, Cambridge CB2 1EZ, UK; fax: (+44) 1223-336-033; or deposit @ccdc.cam.ac.uk).
- [9] The accessible volume is the volume that can be accessed by a given probe from outside the crystal. It was calculated with a 1.4 Å probe radius using Cerius² Version 3.8. **1998**. This program was developed by BIOSYM/Molecular Simulations.
- [10] The geometry of the indole hydrogen bond, $\text{N1E1-H1E1} \cdots \text{O2}^{(i)}$ [$(i) = y, 1 - x, z - 0.25$], changes from N1E1-H1E1 , $\text{H1E1} \cdots \text{O2}^{(i)}$, $\text{N1E1} \cdots \text{O2}^{(i)}$, $\text{N1E1-H1E1} \cdots \text{O2}^{(i)}$ of 0.86, 2.24, 2.925(2) Å, 136° with a standard riding model to 0.86(3), 2.10(3), 2.9247(19) Å, $160(3)^\circ$ at 120 K. Changes are similar at 295 K.
- [11] T. J. Emge, A. Agrawal, J. P. Dalessio, G. Dukovic, J. A. Inghrim, K. Janjua, M. Macaluso, L. L. Robertson, T. J. Stiglic, Y. Volovik, M. M. Georgiadis, *Acta Crystallogr. Sect. C* **2000**, *56*, e469–e471.
- [12] Lattice parameters were determined by Le Bail fits: A. Le Bail, H. Duroy, J. L. Fourquet, *Mater. Res. Bull.* **1988**, *23*, 445–452, using GSAS: A. C. Larson, R. B. Von Dreele, *Los Alamos Natl. Lab. Rep. LA (US)* **1994**, LAUR 86–748, after the 2D images had been reduced to 1D powder patterns using FIT2D: a) A. P. Hammersley, **1998**. ESRF Internal Report, ESRF98HA01T, FIT2D V10.3 Reference Manual V4.0; b) A. P. Hammersley, S. O. Svensson, M. Hanfland, A. N. Fitch, D. Häusermann, *High Pressure Res.* **1996**, *14*, 235–248.
- [13] P. Pattison, K. D. Knudsen, R. Cerny, E. Koller, *J. Synchrotron Radiat.* **2000**, *7*, 251–256.

Supramolecular Templating of the Double-Cubane $[\{\text{Cu}_3(\text{Hpz}^{\text{tBu}})_6(\mu_3\text{-Cl})(\mu_3\text{-OH})_3\}_2\text{Cu}]\text{Cl}_6$ ($\text{Hpz}^{\text{tBu}} = 5\text{-tert-Butylpyrazole}$)**

Xiaoming Liu, Judith A. McAllister, Marcelo P. de Miranda, Benjamin J. Whitaker, Colin A. Kilner, Mark Thornton-Pett, and Malcolm A. Halcrow*

While the $[\text{M}_4(\mu_3\text{-X})_4]^{4+}$ ($\text{M} = \text{transition ion}$, $\text{X} = \text{anion or dianion}$) cubane structure is a common motif in transition metal chemistry and biochemistry, only a few examples of vertex-sharing double-cubane compounds are known.^[1–8] We note in particular **1** (bipym = 2,2'-bipyrimidine), which is the only compound with this topology whose magnetochemical properties have been fully elucidated to date.^[5] We report here a new example of a heptacopper double-cubane complex, **2**, whose molecular structure and magnetochemistry differ substantially from those of **1**. Moreover, the unusual structure of **2** is supported by a unique pattern of supramolecular cation:anion interactions.



Turquoise crystals of $\mathbf{2} \cdot 2\text{CH}_2\text{Cl}_2$ were grown from CH_2Cl_2 /pentane mixtures.^[9] The asymmetric unit of these crystals contains half a complex molecule with Cu(1) lying on a crystallographic inversion center, forming a $[\{\text{Cu}_3(\text{Hpz}^{\text{tBu}})_6(\mu_3\text{-Cl})(\mu_3\text{-OH})_3\}_2\text{Cu}]^{6+}$ double-cubane (Figure 1). The shared-vertex Cu(1) is ligated by six OH^- ligands, with an axis of Jahn–Teller elongation along the $\text{O}(7)\text{-Cu}(1)\text{-O}(7')$ vector. The other Cu ions exhibit tetragonal geometries, with two OH^- and two Hpz^{tBu} ligands in the basal plane and axial contacts to two Cl^- ions. Cu(3) and Cu(4) adopt almost identical geometries, with contacts of 2.7949(5)–2.9129(6) Å to Cl(62) and one other Cl^- ligand. However, Cu(2) has a shorter distance of 2.5502(5) Å to Cl(62), and a much longer distance of 3.7433(6) Å to Cl(63) (not shown in Figure 1).

In addition to Cl(62) and its symmetry-generated equivalent, there are six Cl^- ions disposed in a ring around the heptacopper core of the molecule (Figure 2). Each of these Cl^- ions accepts three hydrogen bonds, from one OH^- and two Hpz^{tBu} N–H donors. Cl(64) and Cl(65) are in near-

[*] Dr. M. A. Halcrow, Dr. X. Liu, Dr. M. P. de Miranda, Dr. B. J. Whitaker, C. A. Kilner, Dr. M. Thornton-Pett
School of Chemistry
University of Leeds
Leeds LS2 9JT (UK)
Fax: (+44) 113-233-6565
E-mail: M.A.Halcrow@chem.leeds.ac.uk

Dr. J. A. McAllister
Department of Chemistry
University of Cambridge
Lensfield Road, Cambridge CB2 1EW (UK)
and
Interdisciplinary Research Centre in Superconductivity
University of Cambridge
Madingley Road, Cambridge CB3 0HE (UK)

[**] This work was supported by the Royal Society (London, M.A.H.) and the EPSRC (X.L., J.A.M.).

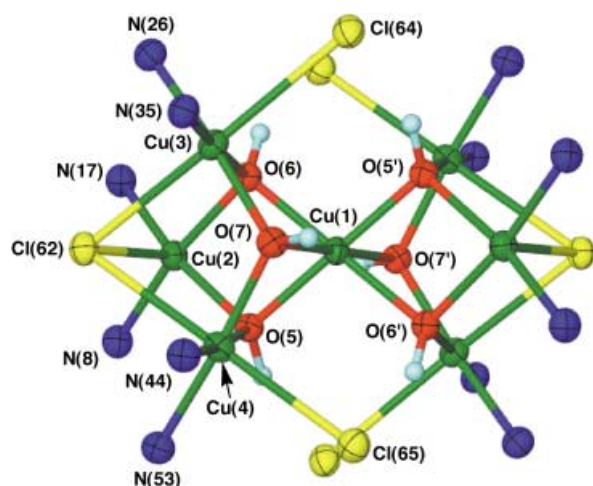


Figure 1. View of the $[\text{Cu}_3(\text{Hpz}^{\text{tBu}})_6(\mu_3\text{-Cl})(\mu_3\text{-OH})_3]_2\text{Cu}^{6+}$ core in the crystal structure of $2 \cdot 2 \text{CH}_2\text{Cl}_2$. For clarity, only the coordinated N atoms of the Hpz^{tBu} ligands are shown. Thermal ellipsoids are at the 50% probability level. Color code: Cu: green; O: red; N: blue; Cl: yellow; H: turquoise. Selected bond lengths [Å] and angles [°]: Cu(1)–O(5) 1.9781(13), Cu(1)–O(6) 1.9675(13), Cu(1)–O(7) 2.2957(13), Cu(2)–O(5) 1.9731(14), Cu(2)–O(6) 1.9862(13), Cu(3)–O(6) 1.9940(13), Cu(3)–O(7) 1.9549(14), Cu(4)–O(5) 2.0076(14), Cu(4)–O(7) 1.9493(13); O(5)–Cu(1)–O(6) 81.00(5), O(5)–Cu(1)–O(7) 99.00(5), O(5)–Cu(1)–O(7) 75.74(5), O(5)–Cu(1)–O(7) 104.26(5), O(6)–Cu(1)–O(7) 76.06(5), O(6)–Cu(1)–O(7) 103.94(5), O(5)–Cu(2)–O(6) 80.66(6), O(6)–Cu(3)–O(7) 83.86(6), O(5)–Cu(4)–O(7) 83.51(6), Cu(1)–O(5)–Cu(2) 96.61(6), Cu(1)–O(5)–Cu(4) 102.33(6), Cu(2)–O(5)–Cu(4) 108.97(6), Cu(1)–O(6)–Cu(2) 96.53(6), Cu(1)–O(6)–Cu(3) 101.59(6), Cu(2)–O(6)–Cu(3) 111.11(6), Cu(1)–O(7)–Cu(3) 92.12(5), Cu(1)–O(7)–Cu(4) 93.65(5), Cu(3)–O(7)–Cu(4) 118.55(7). Primed atoms are related to unprimed atoms by the symmetry operation: $1-x, 1-y, 1-z$.

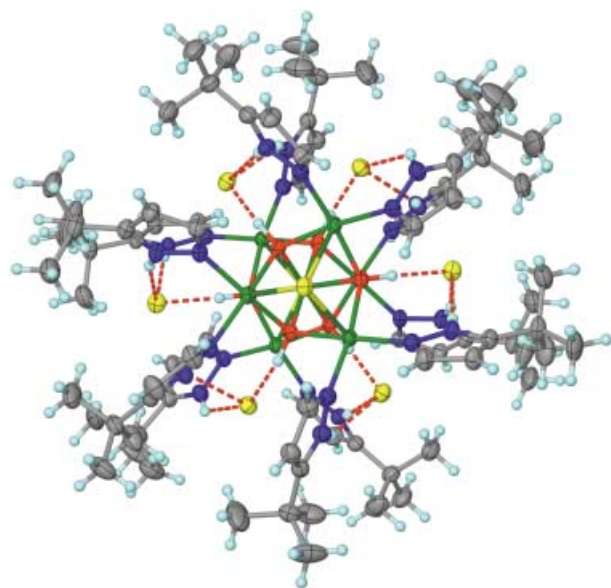


Figure 2. View of the $[\text{Cu}_3(\text{Hpz}^{\text{tBu}})_6(\mu_3\text{-Cl})(\mu_3\text{-OH})_3]_2\text{Cu}\text{Cl}_6$ molecule in the crystal structure of $2 \cdot 2 \text{CH}_2\text{Cl}_2$, showing the hydrogen-bonding interactions to the Cl^- ions. The view is parallel to the $\text{Cl}(62) \cdots \text{Cu}(1) \cdots \text{Cl}(62')$ vector in Figure 1. Color code as for Figure 1 with C: gray.

identical environments 2.8–2.9 Å from the closest Cu ion (see above). However Cl(63), which is hydrogen-bonded to the OH^- ligand O(7') lying on the axis of Jahn–Teller elongation at Cu(1), is displaced from the equivalent site by 0.9 Å away from Cu(2). These hydrogen-bonded Cl^- ions are encapsu-

lated inside the Hpz^{tBu} *tert*-butyl substituents, which enclose the molecule in a hydrophobic sheath.

Magnetic susceptibility data were obtained between 5–330 K from a powder sample of **2**, in an applied field of 2000 G (Figure 3). At 300 K $\chi_{\text{M}}T = 2.4 \text{ cm}^3 \text{ mol}^{-1} \text{ K}$, which is

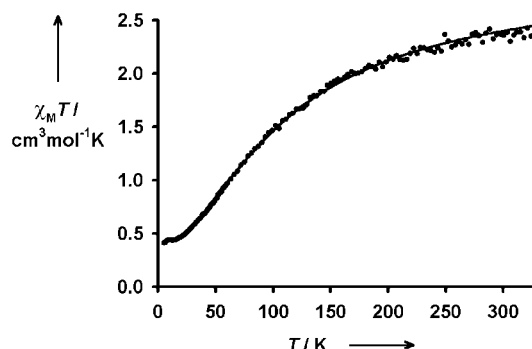
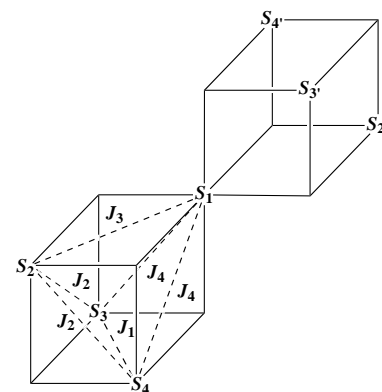


Figure 3. Plot of $\chi_{\text{M}}T$ versus T for a powder sample of **2** (circles), showing the best theoretical fit (line). See text for fitting details.

slightly smaller than the spin-only value expected for seven noninteracting $S = 1/2$ Cu^{II} ions ($2.6 \text{ cm}^3 \text{ mol}^{-1} \text{ K}$).^[10] As the temperature is lowered $\chi_{\text{M}}T$ decreases, reaching a plateau of $0.44 \text{ cm}^3 \text{ mol}^{-1} \text{ K}$ at 15 K which is consistent with a fully populated $S = 1/2$ ground state.^[10] These data were interpreted by using the Hamiltonian in Equation (1) (see Scheme 1 for the exchange-coupling scheme adopted).^[11]

$$H = -2J_1(S_3S_4 + S_3S_4) - 2J_2(S_2S_3 + S_2S_4 + S_2S_3 + S_2S_4) - 2J_3(S_1S_2 + S_1S_2) - 2J_4(S_1S_3 + S_1S_4 + S_1S_3 + S_1S_4) \quad (1)$$

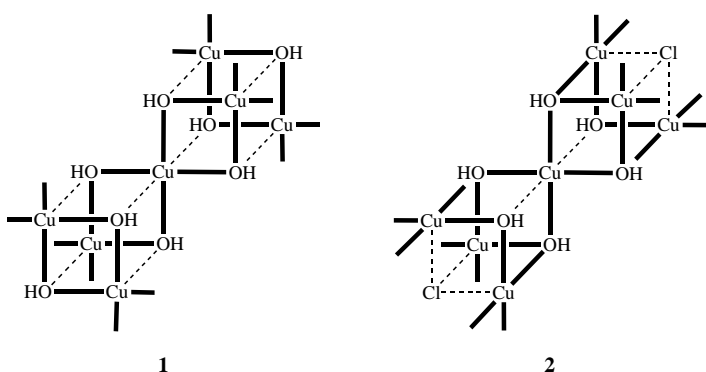


Scheme 1. Exchange-coupling scheme employed to analyze the magnetic data of **2**. Each spin equates to the correspondingly numbered Cu ion in Figure 1 (i.e. $S_1 \equiv \text{Cu}(1)$ etc.).

During the analysis it was found that $J_2 \approx J_4$, and that both of these parameters were poorly defined owing to correlation problems. Therefore, these two J values were constrained to be equal for the final fitting, which yielded $g = 2.14$, $J_1 = -72$, $J_3 = -21$ and $J_2 = J_4 = -16 \text{ cm}^{-1}$ (Figure 3). The constant J_3 describes superexchange mediated by two OH^- ligands that both lie in the xy magnetic planes of Cu(1) and Cu(2). The observed value for this coupling agrees well with Haase's

correlation for basal–basal superexchange in $[\text{Cu}_4(\mu_3\text{-OR})_4]^{4+}$ (R = alkyl) cubanes, which predicts $J_3 \approx -30 \text{ cm}^{-1}$ for the observed average Cu(1)–O–Cu(2) angle of $96.57(8)^\circ$.^[12] The other superexchange constants J_1 , J_2 , and J_4 in **2** are all effectively mediated by $[\text{Cu}_2(\mu\text{-OH})]^{3+}$ bridges, across average Cu–O–Cu angles of $118.55(7)^\circ$, $110.04(8)^\circ$, and $101.96(8)^\circ$, respectively. This is consistent with J_1 being more antiferromagnetic than J_2 or J_4 .^[12, 13] Since J_1 is the strongest antiferromagnetic coupling in the molecule, this means that Cu(1), Cu(2), and Cu(2') are spin-frustrated with respect to Cu(3), Cu(4), Cu(3'), and Cu(4').

While they both have C_s symmetry, the heptacopper cores of **1**^[5] and **2** are very different (Scheme 2). Compound **1** can be described structurally and magnetically as a pair of vertex-linked C_2 -symmetric $[\text{Cu}_4(\text{bipy})_3(\mu_3\text{-OH})_4]^{4+}$ cubanes. This



Scheme 2. Comparative molecular structures of **1** and **2**, showing the basal (thick lines) and apical (dashed lines) Cu–X (X = O, Cl) bonds.

“dimer of dimers” motif is common in $[\text{Cu}_4(\mu_3\text{-OR})_4]^{4+}$ (R = H, alkyl) cubane compounds.^[12, 14] However, the individual $[\text{Cu}_4(\text{Hpz}^{\text{Bu}})_6(\mu_3\text{-Cl})(\mu_3\text{-OH})_3]^{4+}$ cubane moieties in **2** are C_s -symmetric, being distorted from C_{3v} symmetry by the Jahn–Teller elongation at Cu(1). This is the first example of this structural type in Cu^{II} chemistry.

There is a small, but growing, number of compounds containing an enclosed guest anion or cation inside a polyoxometalate^[15] or polynuclear coordination complex^[16] cage. The guest ion in these compounds templates the structure of the surrounding framework, despite interacting with it only through electrostatic and van der Waals interactions. Compound **2** is an inversion of the usual scenario, in that the metal core is encapsulated by a belt of hydrogen-bonded, templating anions. Experiments are in progress to prepare new mono- and bidentate ligands designed as anion receptors, in order to use supramolecular chemistry to prepare other novel metal–oxo or –hydroxo cluster architectures.

Experimental Section

To a mixture of CuCl_2 (0.13 g, 1.0 mmol) in MeOH (30 mL) was added a MeOH (20 mL) solution of NaOH (0.040 g, 1.0 mmol) and 3[5]-*tert*-butylpyrazole (0.24 g, 2.0 mmol). The resultant dark green solution was stirred at 293 K for three days, then evaporated to dryness. Extraction of the residue with CH_2Cl_2 , and layering of the resultant green solution with

pentane, yielded turquoise crystals of **2**. Yield 0.18 g, 54% based on Cu. Elemental analysis calcd (%) for $\text{C}_{84}\text{H}_{150}\text{Cl}_8\text{Cu}_7\text{N}_{24}\text{O}_6$: C 43.47, H 6.51, N 14.49; found: C 43.50, H 6.55, N 14.55.

Received: August 27, 2001

Revised: November 26, 2001 [Z17802]

- [1] M. L. Ziegler, J. Weiss, *Angew. Chem.* **1970**, 82, 931–932; *Angew. Chem. Int. Ed. Engl.* **1970**, 9, 905–906.
- [2] M. Shibahara, T. Yamamoto, H. Kanadani, H. Kuroya, *J. Am. Chem. Soc.* **1987**, 109, 3495–3496.
- [3] M. D. Clerk, M. J. Zaworotko, *J. Chem. Soc. Chem. Commun.* **1991**, 1607–1608.
- [4] I. Büsching, H. Strasdeit, *J. Chem. Soc. Chem. Commun.* **1994**, 2789–2790.
- [5] J. A. Real, G. De Munno, R. Chiapetta, M. Julve, F. Lloret, Y. Journeaux, J.-C. Colin, G. Blondin, *Angew. Chem.* **1994**, 106, 1223–1226; *Angew. Chem. Int. Ed. Engl.* **1994**, 33, 1184–1186.
- [6] W. A. Herrmann, A. Egli, E. Herdtweck, R. Alberto, F. Baumgärtner, *Angew. Chem.* **1996**, 108, 486–489; *Angew. Chem. Int. Ed. Engl.* **1996**, 35, 432–434.
- [7] V. Tangoulis, C. P. Raptopoulou, S. Paschalidou, E. G. Bakalbassis, S. P. Perlepes, A. Terzis, *Angew. Chem.* **1997**, 109, 1165–1167; *Angew. Chem. Int. Ed. Engl.* **1997**, 36, 1083–1085.
- [8] R.-K. Chiang, C.-C. Huang, C.-S. Wur, *Inorg. Chem.* **2001**, 40, 3237–3239.
- [9] Crystal data for $2 \cdot 2\text{CH}_2\text{Cl}_2$: triclinic, $P\bar{1}$, $a = 12.3485(1)$, $b = 15.8875(1)$, $c = 17.6179(2)$ Å, $\alpha = 116.6860(4)$, $\beta = 103.7656(4)$, $\gamma = 91.3234(7)^\circ$, $V = 2965.70(5)$ Å³, $Z = 1$, $\rho_{\text{calcd}} = 1.394 \text{ Mg m}^{-3}$. Data were collected at 150 K on a Nonius KappaCCD diffractometer, $\text{MoK}\alpha$ radiation ($\lambda = 0.71073$ Å), 64587 measured reflections to $2\theta_{\text{max}} = 55.06^\circ$, giving 13553 unique reflections ($R_{\text{int}} = 0.056$). The structure was solved by a Patterson synthesis,^[17] and refined against F^2 using all data.^[18] The solvent molecule is disordered over two orientations, which were modeled using restrained C–Cl bond lengths and 1,3-Cl...Cl distances. The final discrepancy indices were $R_1 = 0.034$, $wR_2 = 0.096$. CCDC-169366 contains the supplementary crystallographic data for this paper. These data can be obtained free of charge via www.ccdc.cam.ac.uk/conts/retrieving.html (or from the Cambridge Crystallographic Data Centre, 12, Union Road, Cambridge CB2 1EZ, UK; fax: (+44) 1223-336-033; or deposit@ccdc.cam.ac.uk).
- [10] C. J. O'Connor, *Prog. Inorg. Chem.* **1982**, 29, 203–283.
- [11] The Hamiltonian matrix was calculated in the coupled-spins representation, in which it can be made block-diagonal. The blocks were independently diagonalized using MAPLE (with the RACAH package for angular momentum algebra),^[19] leading to analytical equations for the energies of their eigenstates and their derivatives. These expressions were used in a nonlinear fit of the van Vleck equation to $\chi_M T$, using an iterative procedure based on the Marquadt method.^[20] No paramagnetic impurity or TIP term was included in the final analysis.
- [12] L. Merz, W. Haase, *J. Chem. Soc. Dalton Trans.* **1980**, 875–879.
- [13] V. H. Crawford, H. W. Richardson, J. R. Wasson, D. J. Hodgson, W. H. Hatfield, *Inorg. Chem.* **1976**, 15, 2107–2110.
- [14] J. Sletten, A. Sørensen, M. Julve, Y. Journeaux, *Inorg. Chem.* **1990**, 29, 5054–5058, and references therein.
- [15] A. Müller, H. Reuter, S. Dillinger, *Angew. Chem.* **1995**, 107, 2505–2539; *Angew. Chem. Int. Ed. Engl.* **1995**, 34, 2328–2361.
- [16] S. Leininger, B. Olenyuk, P. J. Stang, *Chem. Rev.* **2000**, 100, 853–908.
- [17] G. M. Sheldrick, SHELXS 97, University of Göttingen, **1997**.
- [18] G. M. Sheldrick, SHELXL 97, University of Göttingen, **1997**.
- [19] S. Fritzsche, T. Inghoff, T. Bastug, M. Tomaselli, *Comput. Phys. Commun.* **2001**, 139, 314–326.
- [20] W. H. Press, S. A. Teukolsky, W. T. Vetterling, B. P. Flannery, *Numerical Recipes: the Art of Scientific Computing*, Cambridge University Press, Cambridge, UK, **1992**.